A&A 509, A21 (2010)
DOI: 10.1051/0004-6361/200913332


Astronomy & Astrophysics

# First spectroscopic analysis of $\beta$ Scorpii C and $\beta$ Scorpii E

## Discovery of a new HgMn star in the multiple system $\beta$ Scorpii

G. Catanzaro

INAF - Osservatorio Astrofisico di Catania, via S. Sofia 78, 95123 Catania, Italy
e-mail: gca@oact.inaf.it

Received 21 September 2009 / Accepted 8 October 2009

**ABSTRACT**

*Context.* The multiple system $\beta$ Scorpii consists of five components and two suspected members forming a total of seven stars. In the past, this system acquired much interest because of a series of occultation by the planet Jupiter and one of its satellites (Io). The study of this phenomena allowed us to ascertain the principal components of the system and the possible nature of each component.
*Aims.* By using optical spectroscopy, we derive radial velocities, $T_{\rm eff}$, $\log g$, abundances $L/L_{\odot}$, $M/M_{\odot}$, and $R/R_{\odot}$ for $\beta$ Sco C and E. We also refine previously published values of $L/L_{\odot}$, $M/M_{\odot}$, and $R/R_{\odot}$ of $\beta$ Sco Aa + Ab to obtain a clear understanding of the evolutionary state of the $\beta$ Sco system.
*Methods.* We convert Doppler shifts in wavelength into radial velocities. Atmospheric parameters and abundances are computed by assuming the local thermodynamic equilibrium using model atmospheres and the spectral synthesis codes ATLAS and SYNTHE.
*Results.* We solve the orbit of $\beta$ Sco E and provide information about the motion of $\beta$ Sco C. By fitting four Balmer lines, we determine that: $T_{\rm eff}^{\rm C} = 24\,000 \pm 500$ K, $\log g^{\rm C} = 3.8 \pm 0.2$, and $T_{\rm eff}^{\rm Ea} = 13\,000 \pm 800$ K, $\log g^{\rm Ea} = 4.2 \pm 0.2$. Rotational velocities are derived by modeling the profiles of metallic lines: $v \sin i^{\rm C} = 55 \pm 3$ km s$^{-1}$ and $v \sin i^{\rm Ea} = 5 \pm 1$ km s$^{-1}$. As for the abundances, we find that $\beta$ Sco C is more or less of solar abundance, while $\beta$ Sco Ea has a significant overabundance of manganese, followed by those of strontium, phosphorous, and titanium. The most underabundant element is magnesium, followed by silicon, aluminum, sulfur, iron, and nickel. Other light elements, such as carbon, nitrogen, oxygen, and neon, are found to be normal. From the derived values of luminosities and temperatures, we infer that these stars have an age of $\approx$6.3 $\pm$ 3.0 Myr.
*Conclusions.* We explain the observed variability in velocity of $\beta$ Sco E in terms of a close companion. Thus, we observe a triple system composed by $\beta$ Sco C and $\beta$ Sco Ea + Eb. While $\beta$ Sco C is a normal star, $\beta$ Sco Ea is probably a mercury-manganese (HgMn) star. The line-profile variability observed for $\beta$ Sco C could be explained by assuming its membership to the class of slow pulsating B stars. According to the position of $\beta$ Sco Ab in the HR diagram, we exclude the possibility that this star could be a $\beta$ Cephei class pulsator.

**Key words.** stars: individual: $\beta$ Scorpii – binaries: spectroscopic – stars: abundances – stars: chemically peculiar

## 1. Introduction

$\beta$ Scorpii is one of the most remarkable multiple systems in all the northern sky. Its components have been studied extensively since 1964, when a sequence of occultations by planet Jupiter occurred. The most detailed description of the system was given by Van Flandern & Espenschied (1975) and a couple of years later by Evans et al. (1977). After these studies, no additional observations have been made.

Before continuing, we summarize the properties of the system and the nomenclature of its component. Component A is HD 144217 (HR 5984), a B0.5 $V$ star with $V = 2.62$ (Nicolet 1978). It was found by Abhyankar (1959) to be a spectroscopic binary (Aa + Ab) with $\Delta m = 1.26$ (Elliot et al. 1976) and an orbital period of 6.828245 ± 0.000009 days (Holmgren at al. 1997). Components Aa + Ab have a more distant companion, the B component. It has been a visual companion since the middle of the last century when its slow orbital motion brought it too close to A for visual separation. According to Evans et al. (1977), the separation between A and B is approximately of 0.394 arcsec. Van Flandern & Espenschied (1975) also detected a possible spectroscopic companion to B, on the basis that the B component should have a mass greater than that deduced from its assumed absolute magnitude, to ensure the dynamical stability of the system. However, this component (G) has yet to be confirmed.

Holmgren at al. (1997) studied $\beta$ Sco A in detail with the twofold purpose of searching for line profile variability (LPV) and to provide more accurate physical parameters of the components. They found for Aa and Ab, respectively, the following atmospheric parameters: $T_{\rm Aa} = 28\,000 \pm 2000$ K and $\log g_{\rm Aa} = 3.95 \pm 0.33$ (B0.5IV-V), $T_{\rm Ab} = 26\,400 \pm 2000$ K and $\log g_{\rm Ab} = 4.20 \pm 0.35$ (B1.5 V). They also proposed that $\beta$ Sco Ab could be a $\beta$ Cep-type star, since they claimed a possible LPV detection with a period of 0.17333 days. Finally, from their analysis the authors suggested the presence of eclipses.

Far from the A component, the component C (HD 144218 = HR 5985) lies at a distance estimated by Van Flandern & Espenschied (1975) to be 13.6 arcsec; it is a B2 V star with $V = 4.92$ (Johnson & Morgan 1953). The analysis used to study data for the occultation by the Jupiter satellite Io, found this star to be double, its E component with a difference of 2.1 mag (Evans et al. 1977) having a very close separation of $\approx$0.1 arcsec (Bartholdi & Owen 1972; Hubbard & Van Flandern 1972). Basing their argument on its unusual colors, Van Flandern & Espenschied (1975) suggested that this component should itself be double, and proposed that its

hypothetical companion as F, or alternatively that it could be a peculiar star with no additional companion.

The orbital elements of the visual couples AB (BU 947AB) and CE (McA 42CE) were computed for the first time by Seymour et al. (2002), who found periods of 610 yrs and 28.1 yrs, respectively. These authors stated that the orbits of two-component pairs of this complex system were calculated independently of each another and a multibody solution was not attempted.

For the CE pair, no detailed spectroscopic analysis has yet been performed to our knowledge. The aim of this paper is to characterize these two stars, their motions and their atmospheres, deriving their effective temperatures, gravities, and abundances. In particular, this study will allow us to draw some important conclusions about the possible presence of the F companion. Further, because of the Holmgren at al. (1997) parallaxes, we could refine the astrophysical quantities such as: $L/L_{\odot}$, $M/M_{\odot}$, and $R/R_{\odot}$, of all the principal four components of $\beta$ Sco system, and we discuss the Holmgren at al. (1997) hypothesis regarding the membership of $\beta$ Sco Ab to the class of $\beta$ Cephei pulsators.

## 2. Observations and data reduction

The spectra used in our analysis were acquired with different equipments:

- a spectrum of $\beta$ Sco C + E was downloaded from the ESO archive. In particular, this spectrum was acquired with FEROS@MPI-2.2 m on May 3, 2004 at La Silla Observatory, Chile. The signal-to-noise ratio was always higher than 150. The spectral resolution was $R = 48\,000$.
- Spectrum of the pair $\beta$ Sco C + E were downloaded from the CFHT archive. This spectrum was acquired on May 20, 2005 with ESPADONS mounted on the 3.6 m and covers a wavelength region from 3750 to 9200 Å, a signal-to-noise ratio always greater than 300. Because of the strong contamination by telluric lines and the presence of fringes, we limited our analysis to the interval between 3700 Å and 7000 Å. Resolving power is ≈70 000, as derived from emission lines of the Th-Ar calibration lamp.
- The 91 cm telescope of the *INAF - Osservatorio Astrofisico di Catania* (OAC), was used by ourselves to acquire 13 spectra of $\beta$ Sco C + E. The telescope is fiber-linked to a REOSC echelle spectrograph, which allows us to obtain $R = 20\,000$ spectra in the range 4300–6800 Å. The resolving was measured using emission lines of the Th-Ar calibration lamp. Spectra were recorded on a thinned, back-illuminated (SITE) CCD with 1024×1024 pixels of 24 $\mu$m size, a typical readout noise of 6.5 $e^-$, and a gain of 2.5 $e^-$/ADU.

All these spectra were calibrated in wavelength with the continuum normalized to unity, by using standard data reduction procedures for spectroscopic observations within the NOAO/IRAF package. IRAF package *rvcorrect* was used to include the velocity correction required because of the Earth's motion, and all the spectra were then transformed into a heliocentric rest frame.

## 3. Radial velocities and orbital parameters

In our highest resolution spectra (i.e., CFHT and ESO), the lines of the E component are easily detected at a wide range of wavelengths. Unfortunately, because of their lower resolution, in the OAC data we identified the lines of that component only in the limited fraction of the spectral range between 4545 Å and 4580 Å. In particular, we identified 5 lines, namely: CrII $\lambda$4558.650 Å, TiII $\lambda$4563.757, TiII $\lambda$4571.971, FeII $\lambda$4583.837, and CrII $\lambda$ 4588.199. For each of these lines, we measured the central wavelength with a Gaussian fit of the profile and computed the radial velocity using the classical Doppler shift formula. Velocities are reported in Table 1.

**Table 1.** Radial velocities derived from our spectra.

| HJD (2 450 000.0 +) | $RV_C$ (km $s^{-1}$) | $RV_E$ (km $s^{-1}$) | Obs. |
|---|---|---|---|
| 3128.7485 | −3.45 ± 1.57 | −31.84 ± 0.90 | ESO |
| 3510.8674 | 5.00 ± 0.80 | −18.00 ± 0.70 | CFHT |
| 4616.6065 | −8.32 ± 1.00 | –[a] | OAC |
| 4654.3575 | −8.67 ± 0.30 | −25.00 ± 3.02 | OAC |
| 4655.4475 | −9.08 ± 0.46 | −30.60 ± 1.50 | OAC |
| 4994.3361 | −10.40 ± 1.26 | +28.00 ± 3.00 | OAC |
| 4995.3501 | −7.91 ± 0.69 | +0.00 ± 3.00 | OAC |
| 5005.3340 | −6.00 ± 0.56 | +30.00 ± 3.00 | OAC |
| 5010.3693 | −7.75 ± 0.46 | −22.00 ± 3.00 | OAC |
| 5011.3910 | −7.34 ± 0.54 | −10.00 ± 3.00 | OAC |
| 5018.3175 | −8.29 ± 0.79 | −25.00 ± 3.00 | OAC |
| 5020.3439 | −8.22 ± 0.59 | −35.00 ± 3.00 | OAC |
| 5044.3308 | −8.14 ± 0.28 | −5.00 ± 3.00 | OAC |
| 5045.3084 | −7.43 ± 0.35 | +18.00 ± 3.00 | OAC |
| 5046.2941 | −6.57 ± 0.40 | +37.00 ± 3.00 | OAC |

[a] SNR too low to detect the E component spectral lines.

**Table 2.** Orbital parameters calculated for the E components.

| | |
|---|---|
| $T$ | 2 453 124.11 ± 0.08 |
| $P$ | 10.6851 ± 0.0006 days |
| $e$ | 0.25 ± 0.04 |
| $\gamma$ | −3.2 ± 1.3 |
| $K$ | 37.5 ± 2.1 km $s^{-1}$ |
| $\omega$ | 28 ± 3 degrees |
| $a \sin i$ | 7.7 ± 0.5 $R_{\odot}$ |
| $f$(m) | 0.05 ± 0.01 $M_{\odot}$ |

The radial velocities of a spectroscopic binary system are linked to the orbital parameters by the relation:

$$V_{\rm rad} = \gamma + K[\cos(\theta + \omega) + e\cos\omega], \quad (1)$$

where $\gamma$ is the radial velocity of the center of mass, $e$ is the eccentricity of the orbit, $\omega$ is the longitude of the periastron, $\theta$ is the angular position of the star measured from the center of mass at a given instant, and $K$ is the semi-amplitude of the velocity curve given by the formula

$$K = \frac{2\pi a \sin i}{P\sqrt{1-e^2}}, \quad (2)$$

where $P$ is the orbital period of the system. Orbital elements were determined by a least-square fit to Eq. (1). Errors were estimated from the variation in the parameters which increases the $\chi^2$ of a unit. The starting value for $P$ was evaluated using the *phase dispersion method* (Stellingwerf 1978) developed within the NOAO/IRAF package. The orbital parameters deducted by fitting radial velocities of $\beta$ Sco E are reported in Table 2 and plotted against observations in Fig. 1.

Regarding $\beta$ Sco C, we were unable to fit the data to Eq. (1) and noted that the OAC data infers, within the experimental errors, the same velocity, whose average value is $\langle V_{\rm rad}\rangle = -7.9 \pm 1.0$.

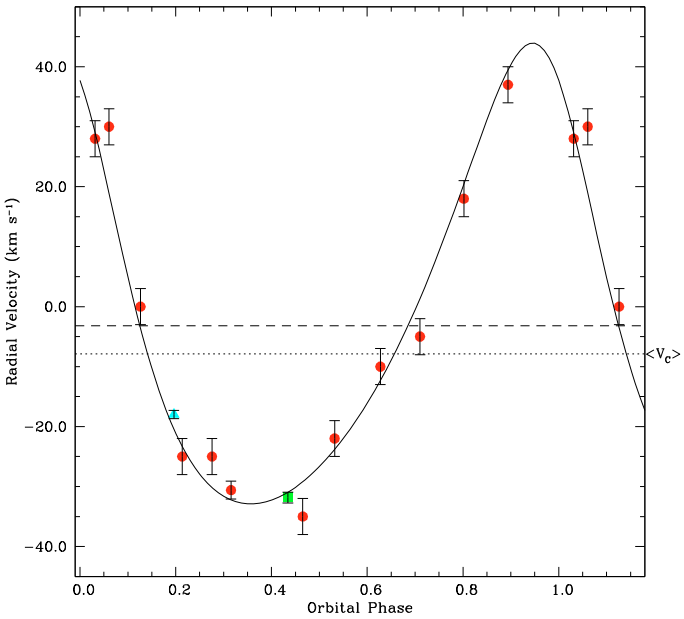


**Fig. 1.** Radial velocity curves of $\beta$ Sco E. Solid line represents the orbital solution, symbols used to represent the data are: circle (red) for OAC, triangle (cyan) for CFHT, and square (green) for ESO. The dashed line is the $\gamma$ velocity, while the dotted line represents the average velocity computed for $\beta$ Sco C

The visual couple CE, also known as McA 42CE, has an orbital period of ~28.1 yrs (Seymour et al. 2002). We found that the E component has an orbital motion with a $P = 10.6851$ days. Thus, these results could be interpreted in the framework of a new scenario, in which the C component is physically linked to a close binary system consisting of $\beta$ Sco Ea + Eb.

## 4. Atmospheric parameters of the components

The approach that we used in this study to determine $T_{\rm eff}$ and $\log g$ of $\beta$ Sco C and $\beta$ Sco Ea, was applied in Catanzaro & Leone (2006) to the triple system 74 Aqr. It consists of comparing the observed and theoretical profiles of all Balmer lines available in our spectra by minimizing the goodness-of-fit parameter

$$\chi^2 = \frac{1}{N}\sum\left(\frac{I_{\rm obs} - I_{\rm th}}{\delta I_{\rm obs}}\right)^2$$

where $N$ is the total number of points, $I_{\rm obs}$ and $I_{\rm th}$ are, respectively, the intensities – normalized to the continuum – of the observed and computed profiles, and $\delta I_{\rm obs}$ is the photon noise. Errors in $T_{\rm eff}$ and $\log g$ are estimated to be the variation in the parameters, which increases the $\chi^2$ of the fitting process of a unit.

The synthetic spectrum normalized to the unity level was derived using the formula

$$F_{\rm Tot} = \frac{F_{\rm C} + F_{\rm Ea}}{I_{\rm C} + I_{\rm Ea}},$$

where $F_{\rm C,Ea}$ and $I_{\rm C,Ea}$ are, respectively, computed fluxes and continua of each component.

Theoretical single profiles were computed with SYNTHE (Kurucz & Avrett 1981) on the basis of ATLAS9 (Kurucz 1993) atmosphere models. All models were evaluated for a solar opacity distribution function and microturbulence velocity $\xi = 2$ km s$^{-1}$. To reduce the number of free parameters, we first determined the rotational velocities of $\beta$ Sco C and Ea by matching metal lines to synthetic profiles in our highest resolution (CFHT) spectra. The best-fit occurred for the values reported in Table 3.

**Table 3.** Atmospheric parameters adopted in our study for the components of our system.

| Star | $v \sin i$ (km s$^{-1}$) | $T_{\rm eff}$ (K) | $\log g$ |
|---|---|---|---|
| $\beta$ Sco C | $55 \pm 3$ | $24\,000 \pm 500$ | $3.8 \pm 0.2$ |
| $\beta$ Sco Ea | $5 \pm 1$ | $13\,000 \pm 800$ | $4.2 \pm 0.2$ |

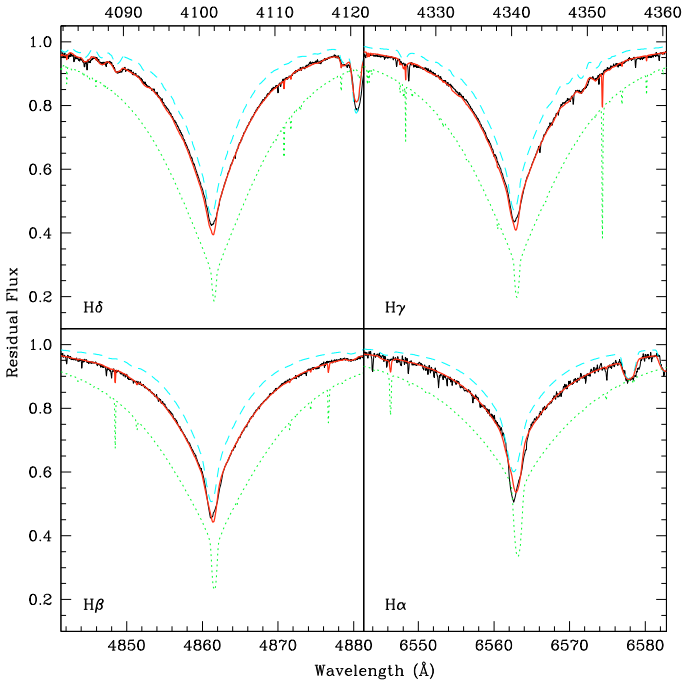


**Fig. 2.** Comparison between observed (CFHT) and computed Balmer line profiles. The synthetic total profile is the combination of $\beta$ Sco C (cyan dashed line) and $\beta$ Sco E (green dotted line).

For our purpose, we used only the *CFHT* spectrum, which is the one of the highest resolution and signal-to-noise ratio (SNR) among our data. We extracted four Balmer lines, namely H$\delta$, H$\gamma$, H$\beta$, and H$\alpha$, where the SNR measured in the continuum next to the wings varies from 250 to 300.

The results obtained by applying this procedure are presented in Table 3 and displayed in Fig. 2. The values obtained for the C component agree with the B2V classification reported in literature.

## 5. Abundance analysis

To derive chemical abundances, we undertook a synthetic modeling of the observed spectrum. This is because of the intrinsic difficulty in determining the true equivalent widths of metal lines that are strongly reduced by the dilution effect caused by the superposition of the fluxes of the components.

In practice, we divided the entire spectral range covered by our data into a number of subintervals each of 20 Å wide. For each interval, we derived the abundances by a $\chi^2$ minimization of the difference between the observed and synthetic total spectrum. Line lists and atomic parameters used in our modeling are

**Table 4.** Abundances derived for $\beta$ Sco C + Ea expressed in term of $\log N(\mathrm{el})/N_{\mathrm{tot}}$ compared with the solar values of Asplund et al. (2005).

| El | $\log N_{\mathrm{el}}/N_{\mathrm{Tot}}$ $\beta$ Sco C | $\log N_{\mathrm{el}}/N_{\mathrm{Tot}}$ $\beta$ Sco E | Sun |
|---|---|---|---|
| C | −3.86 ± 0.16 | −3.70 ± 0.20 | −3.64 |
| N | −4.44 ± 0.12 | −4.60 ± 0.20 | −4.25 |
| O | −3.67 ± 0.13 | −3.50 ± 0.20 | −3.37 |
| Ne | −3.58 ± 0.21 | −3.96 ± 0.20 | −4.19 |
| Mg | −4.09 ± 0.14 | −6.00 ± 0.20 | −4.50 |
| Al | −5.83 ± 0.06 | −6.50 ± 0.20 | −5.66 |
| Si | −4.54 ± 0.23 | −5.82 ± 0.21 | −4.52 |
| P | −6.75 ± 0.07 | −6.17 ± 0.04 | −6.67 |
| S | −4.98 ± 0.19 | −5.70 ± 0.20 | −4.89 |
| Sc | – | −9.20 ± 0.20 | −8.98 |
| Ti | – | −6.72 ± 0.15 | −7.13 |
| Cr | – | −6.35 ± 0.17 | −6.39 |
| Mn | – | −4.91 ± 0.19 | −6.64 |
| Fe | −4.92 ± 0.16 | −5.54 ± 0.15 | −4.58 |
| Ni | – | −6.45 ± 0.07 | −5.80 |
| Sr | – | −8.32 ± 0.21 | −9.11 |

taken from Kurucz & Bell (1995) and the subsequent update by Castelli & Hubrig (2004).

In Table 4, we report the abundances derived in our analysis expressed in the usual logarithmic form relative to the total number of atoms $N_{\mathrm{tot}}$. To easily compare the chemical pattern of $\beta$ Sco C + E, we report in the last column the solar abundances taken from Asplund et al. (2005)[1]. Error reported in Table 4 for a given element is the standard deviation of the average computed among the various abundances determined in each subinterval. When a given element appears in one or two sub-intervals only, the error in its abundance evaluated by varying temperature and gravity in the ranges $[T_{\mathrm{eff}} \pm \delta T_{\mathrm{eff}}]$ and $[\log g \pm \delta \log g]$ is typically 0.20 dex. The abundances of both objects are displayed in Fig. 3.

To check the accuracy of our $T_{\mathrm{eff}}$ and $\log g$ values determined for the C component, we could consider the consistency of the abundances derived from spectral lines of silicon in the first two stages of ionization: −4.64 ± 0.24 for SiII and −4.44 ± 0.19 for SiIII.

In the following sections, we discuss the abundances derived for each component. For each star, we comment on the results for light elements (from carbon to sulfur), iron-group elements (from scandium to nickel) and heavy elements, if any. Regarding helium, spectral lines of the two components are so strongly blended to each other that the measurement of its abundance is impossible.

### 5.1. $\beta$ Sco C

Regarding the light elements reported in Table 4, we did not find any particular peculiarity, only a very slight overabundance of neon and magnesium (≈0.5 dex each).

For what that concerns iron-group elements, we found spectral lines of iron that led to an abundance of −4.92 ± 0.16, slightly beneath the solar value.

Thus, on the basis of our analysis we conclude that this object can be considered as a normal star, as can easily be noted in Fig. 3.

[1] To ensure that these values are directly comparable with our abundances, we changed the scale $\log(N_{\mathrm{elem}})$ relative to $\log(N_{\mathrm{H}}) = 12$, to the scale relative to $\log(N_{\mathrm{tot}})$.

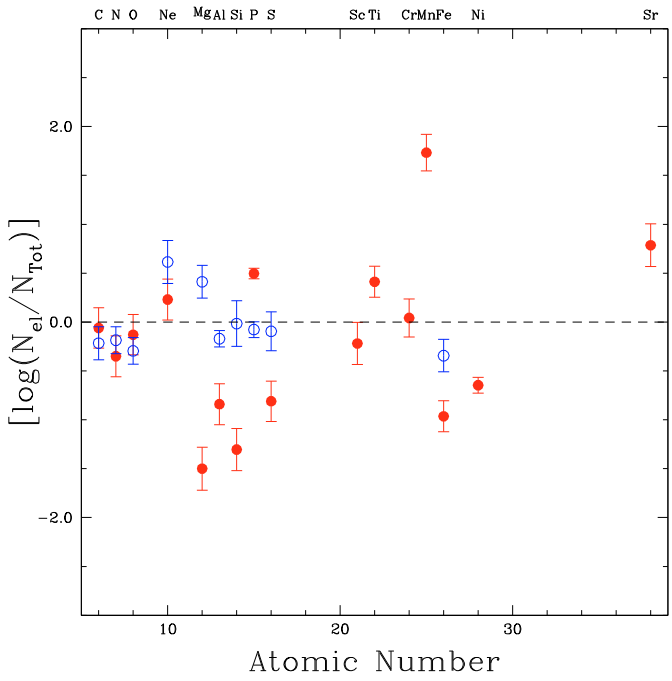


**Fig. 3.** Abundance patterns for the two components. Open circles (blue) represent the pattern of the C component, filled circles (red) are relative to the Ea component.

From a visual examination of the spectra in the SiIII triplet region, we noted a clear line-profile variation similar to those expected for radial and non-radial pulsations. As an example, we show in Fig. 4 the SiIII $\lambda\lambda$ 4567–4574 Å lines for five spectra taken from our sample. To make this comparison possible, we deconvolved the highest resolution data (ESO and CFHT) to the resolution of the OAC resolving power spectra. We attempt to provide an interpretation of this phenomenon in Sect. 7.

### 5.2. $\beta$ Sco Ea

Carbon, nitrogen and oxygen were found to have normal abundances, in addition to neon. Strong underabundances, between 1.0 and 1.5 dex, were found for magnesium, aluminum, silicon, and sulfur, while phosphorus shows an abundance of 0.5 dex greater than the solar case.

For iron-group elements, we found solar abundances for only scandium and chromium. Overabundances were inferred for both titanium (slight, ≈0.5 dex) and manganese (strong, ≈2.0 dex). Only iron and nickel have abundances of below solar, ≈1.0 and ≈0.8 dex, respectively.

In our spectrum, we inferred the presence of only one element heavier than nickel, i.e., strontium, for which an overabundance of ≈0.8 dex was computed.

The chemical pattern of the E component is very complicated, as the reader can see in Fig. 3. It seems to combine a number of abundance anomalies that usually appear in various classes of chemically peculiar stars.

The first hypothesis is that we are dealing with a HgMn star, since it shows clear overabundances of manganese and strontium. Unfortunately, the HgII 3984 Å line, which is the principal indicator of this class of peculiarity, is confused with a much stronger blend (OII 3982.714 plus SiII 3983.722 Å) belonging to the component C. This allow us to estimate only an upper limit

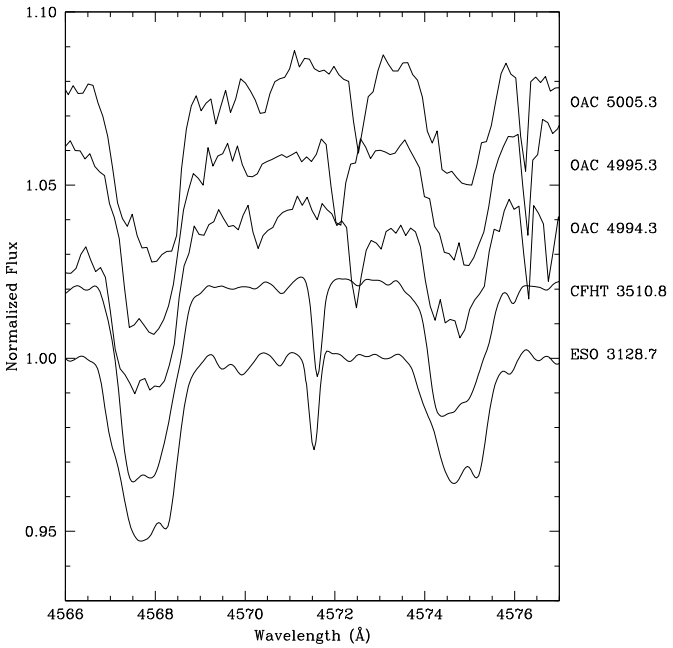


**Fig. 4.** Example data of the SiIII 4567 and 4574 Å of $\beta$ Sco C, with the spectra offset according to acquisition time. For the sake of the comparison, both CFHT and ESO spectra have been deconvolved to the OAC resolution. The moving narrow line is the TiII $\lambda$4571.971 belonging to the E components.

to the mercury overabundance of ≈3.5 dex, otherwise the line would have been detected.

On the other hand, underabundance of elements such as magnesium, silicon, phosphorous, and iron, are typical of other classes of peculiarity, such as $\lambda$ Boo stars for instance, rather than HgMn stars.

## 6. Fundamental astrophysical quantities

The parallax found by Holmgren at al. (1997) for the Aa + Ab pair provides us with the opportunity to refine the positions of these fours stars on the HR diagram. Moreover, since $\beta$ Sco C and $\beta$ Sco Ea belong to the same stellar system, we also adopted the same distance for these two stars.

For the effective temperatures, we adopted those estimated in the study of $\beta$ Sco C and $\beta$ Sco Ea and those published by Holmgren at al. (1997) for the pair Aa + Ab, that is $T_{\rm Aa} = 28\,000 \pm 2000$ K and $T_{\rm Ab} = 26\,400 \pm 2000$ K.

We determine their luminosities on the basis of: visual magnitudes taken from Holmgren at al. (1997) for Aa + Ab and from Mason et al. (2001) for the C + Ea couple; the Sun's bolometric magnitude $M^{\odot}_{\rm bol} = 4.74$ (Drilling & Landolt 1999); the BC from the calibrations published by Flower (1996); and the extinction coefficients $A_v$ of de Geus et al. (1989). Input data and the obtained luminosities are reported in Table 5.

The absolute radii reported in Table 5 were estimated as follows: for the components Aa, Ab, and C we directly combined the angular diameters measured by Elliot et al. (1976) and Elliot et al. (1975) with the adopted distance, while for the Ea components, since no direct measurement of its angular size is available in the literature, we estimated the radius using both the luminosity and effective temperature.

The mass-luminosity relation of main-sequence stars, $\log M/M_{\odot} = 0.48 - 0.105\, M_{\rm bol}$ (Drilling & Landolt 1999), has been used to derive the mass of each component.

**Table 5.** Astrophysical quantities for the $\beta$ Sco System.

| Star | Aa | Ab | C | Ea |
|---|---|---|---|---|
| $A_v$ | $0.55 \pm 0.03$ | | $0.58 \pm 0.03$ | |
| $V$ | 2.62 | 3.88 | 4.52 | 6.60 |
| $M_v$ | $-3.92 \pm 0.05$ | $-2.60 \pm 0.05$ | $-1.83 \pm 0.05$ | $0.24 \pm 0.05$ |
| BC | $-2.7 \pm 0.2$ | $-2.5 \pm 0.2$ | $-2.3 \pm 0.2$ | $-0.9 \pm 0.2$ |
| $M_{\rm bol}$ | $-6.6 \pm 0.2$ | $-5.1 \pm 0.2$ | $-4.1 \pm 0.2$ | $-0.6 \pm 0.2$ |
| $L/L_{\odot}$ | $4.5 \pm 0.1$ | $3.9 \pm 0.1$ | $3.5 \pm 0.1$ | $2.1 \pm 0.1$ |
| $R/R_{\odot}$ | $6.3 \pm 0.5$ | $4.0 \pm 0.3$ | $2.9 \pm 0.5$ | $2.4 \pm 0.1$ |
| $M/M_{\odot}$ | $15.0 \pm 0.7$ | $10.4 \pm 0.5$ | $8.2 \pm 0.4$ | $3.5 \pm 0.2$ |

Distances are expressed in parsecs, while luminosities are in logarithmic form.

With our values of $T_{\rm eff}$ and $L$, we constructed the HR diagram showed in Fig. 6. A comparison with the evolutionary tracks of Bressan et al. (1993), computed for $Z = 0.02$ (solar metalicity), and with isochrones computed by Bertelli et al. (1994) indicates for the $\beta$ Sco system an age of ≈6.3 ± 3.0 Myr, which agrees with the value found by Giannuzzi (1983).

## 7. Discussion and conclusion

The present study represents the first ever quantitative spectroscopic analysis of the stars $\beta$ Sco C and $\beta$ Ea. By using ATLAS9 models with $T_{\rm eff} = 24\,000$ K, $\log g = 3.8$ for $\beta$ Sco C, and $T_{\rm eff} = 13\,000$ K, $\log g = 4.2$ for $\beta$ Sco Ea (both with $\xi = 2$ km s$^{-1}$), we have computed a composite synthetic spectrum and compared it with the observed spectrum. The atmospheric parameters have been computed by a fitting approach that involved at the same time the composite profiles of four Balmer lines, namely: H$\delta$, H$\gamma$, H$\beta$, and H$\alpha$ (see Fig. 2).

According to our analysis, the C component has almost solar metalicity. From the results of the previous section, it can be seen that this component falls into the correct ranges of spectral types and masses to be a suitable candidate *slow pulsating B-star* (SPBs) (Waelkens 1991). This could explain the lines profile variability evident in Fig. 4. Of course, since we do have insufficient data to search for a periodicity, this conclusion needs to be verified by increasing the amount of high resolution spectra at our disposal.

The most puzzling star is certainly component Ea: it exhibits typical characteristics of the HgMn peculiarity class, i.e., strong overabundances of manganese and strontium, but at the same time strong underabundances of other elements such as magnesium, silicon, sulfur, and iron that are usually normal or overabundant in HgMn stars. Nevertheless, this particular chemical composition is not an isolated case in the literature. The pattern that we show in Fig. 3 is very similar to that derived for HR 6000, another HgMn star, studied in detail by Catanzaro et al. (2004) and Castelli & Hubrig (2007). The latter authors tried to explain its peculiarity by considering chemical stratification within the atmosphere. A similar study is difficult to perform in $\beta$ Sco Ea because of the spectral contamination of the C component.

As a final conclusion about their atmospherical parameters, we state that $\beta$ Sco C is a standard star, while $\beta$ Sco Ea is a chemically peculiar object far more likely to belong to the HgMn subgroup.

In Sect. 3, we derived the orbital parameters of $\beta$ Sco Ea (Table 2) by fitting the observed radial velocities to Eq. (1). As we showed there, we were unable to perform the same fitting of $\beta$ Sco C velocities, since the entire set of OAC data do not show any appreciable variability, at least at our resolving power.

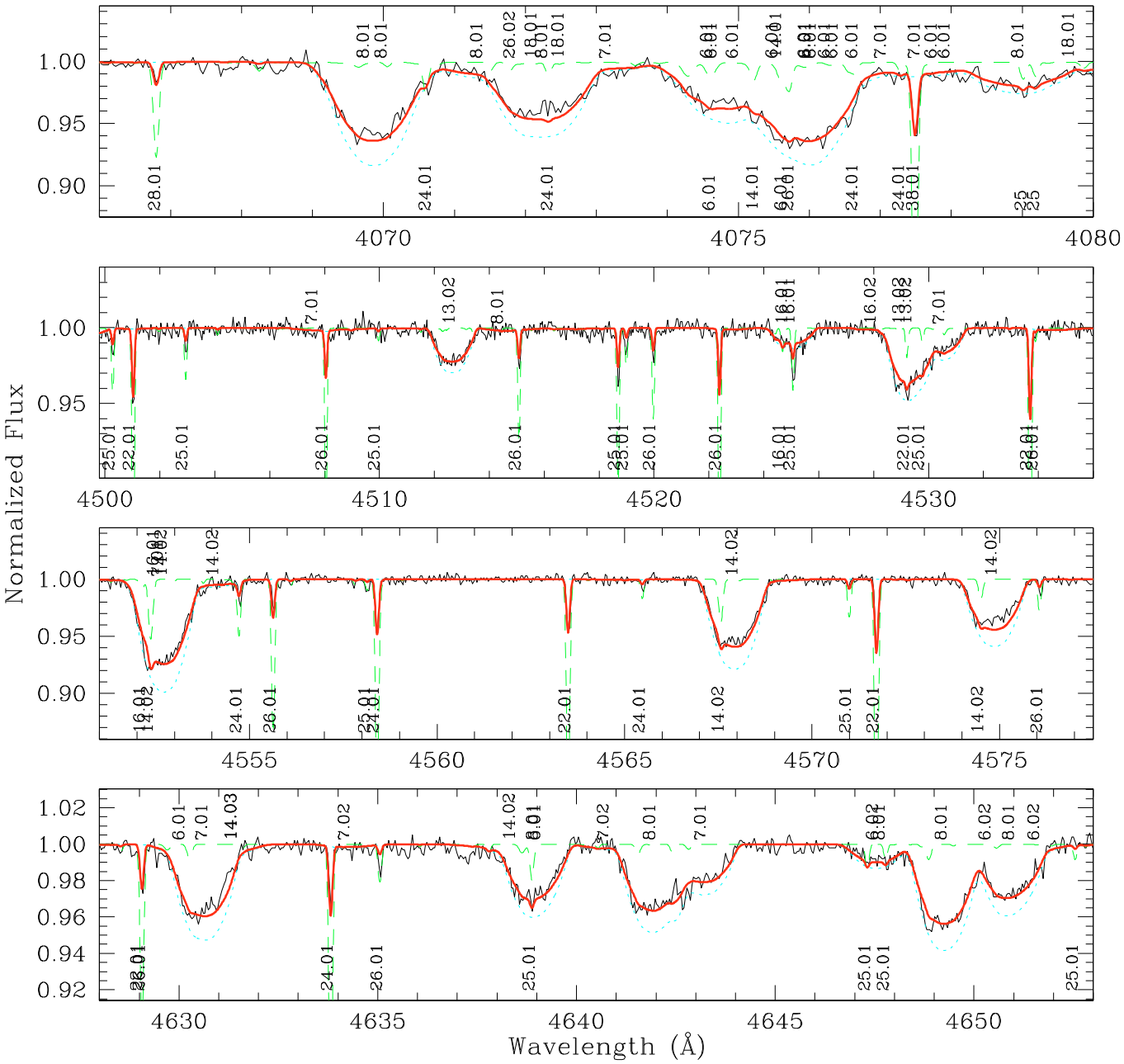


**Fig. 5.** As for example, we show four different intervals of CFHT spectra superimposed on the computed model. Dotted (cyan) line represent the synthetic spectrum computed for the C component, dashed (green) line is the synthetic spectrum calculated for the E component, while the total model is represented by the solid heavy (red) line. In these plots, we also identify the spectral lines with the atomic number and ionization states of the chemical element that generates the line, i.e., 25.01 means MnII. The labels above the spectrum refer to $\beta$ Sco C, while those beneath the spectrum refer to $\beta$ Sco E.

Van Flandern & Espenschied (1975) proposed two explanations of the unusual colors of the E component: a close companion or a very peculiar chemical composition. Our results seem to be in favor of both hypotheses, that is a chemically peculiar star ($\beta$ Sco Ea) with a close companion ($\beta$ Sco Eb).

Holmgren at al. (1997) attempted a preliminary search for line profile variability in the spectral lines of $\beta$ Sco Ab, detecting a possible period of 0.17333 days. They proposed that the star belongs to the class of $\beta$ Cephei pulsators.

$\beta$ Cephei stars are early-B type, near main-sequence objects, which exhibit variations in brightness, radial velocity, and line profiles on timescales of several hours, due to radial and non-radial p- and g-mode pulsations. They are located on the HR diagram in a narrow region where the classic k-mechanism is effective in the partial ionization zone of the iron-group elements. They are in the late stages of core hydrogen-burning phase, just preceding the secondary gravitational contraction (Balona & Engelbrecht 1981). For a clear look at their location inside the instability region, we address the reader to the HR diagram of the confirmed and candidate $\beta$ Cephei stars published by Stankov & Handler (2005).

According to our results, $\beta$ Sco Ab is far from the instability region (see Fig. 6), so we do not confirm the conclusion drawn by previous authors, and, if it exists, the line profile variability has to be ascribed to another origin, such as for example the SPB phenomenon.

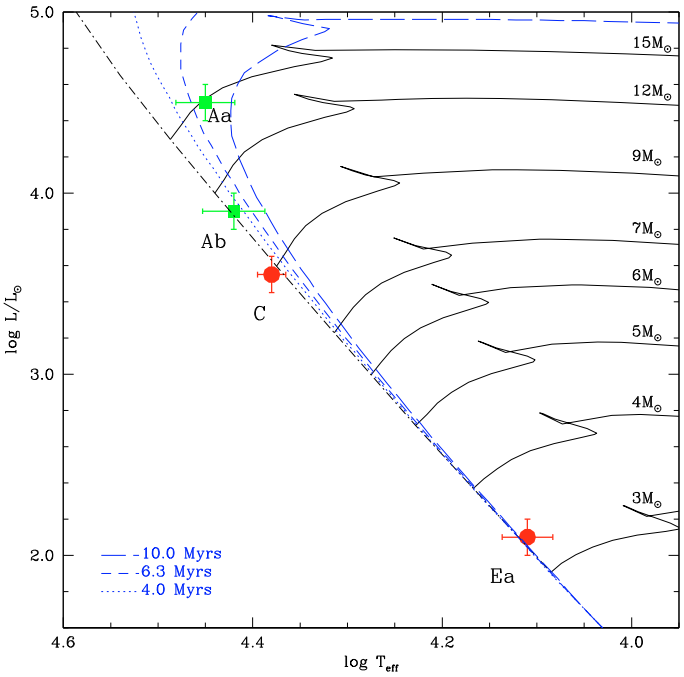


**Fig. 6.** Positions on the HR diagram of the $\beta$ Sco system components: Aa, Ab, C, and Ea. Evolutionary tracks (Bressan et al. 1993) and isochrones (Bertelli et al. 1994) are overplotted.

*Acknowledgements.* This research has made use of the SIMBAD database, operated at CDS, Strasbourg, France. This research has made use of the Washington Double Star Catalog maintained at the US Naval Observatory.
Based on observations made with ESO Telescopes at the La Silla Observatories under programme ID 073.C-0337. This research used the facilities of the Canadian Astronomy Data Centre operated by the National Research Council of Canada with the support of the Canadian Space Agency.
A warm thanks to Anna for her contribution in improving the English form of the manuscript.

## References

Abhyankar, V. D. 1959, ApJS, 4, 157
Asplund, M., Grevesse, N., & Sauval, A. J. 2005, in Cosmic Abundances as Records of Stellar Evolution and Nucleosynthesis, ASP Conf. Ser., 336, 25
Balona, L. A., & Engelbrecht, C. 1981, in Workshop on Pulsating B stars, ed. G. E. V. O. N., & C. Sterken, Nice Observatory, 195
Bartholdi, P., & Owen, F. 1972, AJ, 77, 60
Bertelli, G., Bressan, A., Chiosi, C., Fagotto, F., & Nasi, E. 1994, A&AS, 106, 275
Bressan, A., Fagotto, F., Bertelli, G., et al. 1993, A&AS, 100, 647
de Geus, E. J., de Zeeuw, P. T., & Lub, J. 1989, A&A, 216, 44
Catanzaro, G., & Leone, F. 2006, MNRAS, 373, 330
Catanzaro, G., Leone, F., & Dall, T. H. 2004, A&A, 425, 641
Castelli, F., & Hubrig, S. 2004, A&A, 425, 263
Castelli, F., & Hubrig, S. 2007, A&A, 475, 1041
Drilling, J. S., & Landolt, A. U. 1999, in Allen's Astrophysical Quantities, fourth edition, ed. A. N. Cox, Los Alamos, NM, 381
Elliot, J. L., Wasserman, L. H., Veverka, J., Sagan, C., & Liller, W. 1975, AJ, 80, 323
Elliot, J. L., Rages, K., & Veverka, J. 1976, ApJ, 207, 994
Evans, D. S., Africano, J. L., Fekel, F. C., et al. 1977, AJ, 82, 495
Flower, P. J. 1996, ApJ, 469, 355
Giannuzzi, M. A. 1983, A&A, 125, 302
Johnson, H. L., & Morgan, W. W. 1953, ApJ, 117, 313
Harmanec, P., Hadrava, P., Yang, S., et al. 1997, A&A, 319, 867
Holmgren, D., Hadrava, P., Harmanec, P., Koubský, P., & Kubát, J. 1997, A&A, 322, 565
Hubbard, W. B., & Van Flandern, T. C. 1972, AJ, 77, 65
Kurucz, R. L. 1993, A new opacity-sampling model atmosphere program for arbitrary abundances, in Peculiar versus normal phenomena in A-type and related stars, IAU Coll. 138, ed. M. M. Dworetsky, F. Castelli, & R. Faraggiana, ASP Conf. Ser., 44, 87
Kurucz, R. L., & Avrett, E. H. 1981, SAO Special Rep., 391
Kurucz, R. L., & Bell, B. 1995, Kurucz CD-ROM No. 23, Cambridge, Mass.: Smithsonian Astrophysical Observatory
Nicolet, B. 1978, A&AS, 34, 1
Mason, B. D., Wycoff, G. L., Hartkopf, W. I., Douglass, G. G., & Worley C. E. 2001, AJ, 122, 3466
Seymour, D. M., Mason, B. D., Hartkopf, W. I., et al. 2002, AJ, 123, 1023
Stankov, A., & Handler, G. 2005, ApJS, 158, 193
Stellingwerf, R. F. 1978, ApJ, 224, 953
Van Flandern, T. C., & Espenschied, P. 1975, ApJ, 200, 61
Waelkens, C. 1991, A&A, 246, 453